Enhanced Performance via Partial Lead Replacement by Calcium for $CsPbI_3$ Perovskite Solar Cell exceeding 13% Power Conversion Efficiency

Cho Fai Jonathan Lau, Xiaofan Deng, Jianghui Zheng, Jincheol Kim, Zhilong Zhang, Meng Zhang, Jueming Bing, Benjamin Wilkinson, Long Hu, Robert Patterson, Shujuan Huang, and Anita Ho-Baillie**

Australian Centre for Advanced Photovoltaics, School of Photovoltaic and Renewable Energy Engineering, University of New South Wales, Sydney 2052, Australia

Experiential Section

Device fabrication. Patterned FTO-coated glass (Nippon Sheet Glass, TEC10, 10 $\Omega\,\square^{-1}$) was cleaned by sonication in deionized water with 2 % Hellmanex, acetone and isopropanol for 20 min, respectively. After drying, the substrate was treated by UV ozone cleaner for 20 min. To form the compact TiO_2 blocking layer (c-TiO_2), a solution of titanium diisopropoxide bis(acetylacetonate) in ethanol was deposited on the clean substrate by spray pyrolysis at 450 °C and the substrate was subsequently annealed on a hot plate at 400 °C. After cooling, 150 nm mp-TiO_2 layer was deposited by spin coating Dyesol 30 NR-T paste with a 1:6 dilution in ethanol for 12 s at 4000 rpm. After spin coating, the substrate was dried at 100°C for 10 min and then annealed at 450 °C for 30min. Prior to deposition of perovskite film, the substrate was cleaned by a UVO cleaner for another 20 min and was then transferred to a N_2 filled glovebox. The CsI concentration in the $CsPb_{1-x}Ca_xI_3$ perovskite precursor solution is 1 M, which was prepared by dissolving CsI (Alfa Aesar), PbI_2 (Alfa Aesar) and CaI_2 (Sigma-Aldrich), stoichiometrically in a mixed solvent of dimethylformamide (DMF) (Sigma-Aldrich) and DMSO (Sigma-Aldrich) with a volume ratio of 4:1. The perovskite film was deposited by gas-quenching method (gas assisted spin coating). After the perovskite precursor solution was spread on the mesoporous TiO_2 layer, the substrate was spun firstly at 1000 rpm for 10 s and then 4000 rpm for 30 s. N_2 stream (5.5 bar) was blown over the spinning substrate for 15 s after spinning at 4000 rpm for 5 s. The perovskite film was then annealed at 300 °C for 10 min on a hot plate. The hole transporting solution was prepared by dissolving 10 mg/ml Poly(3-hexylthiophene) (P3HT) (Sigma-Aldrich) in chlorobenzene (Sigma Aldrich) and was deposited on perovskite layer by spin coating at 3000 rpm for 30 s. 100 nm of gold was then thermally evaporated on P3HT to form the top electrode. A cross sectional image of a typical device at high magnification is shown in Figure S1. Finally, the

device was encapsulated using polyisobutene (PIB).[1] For anti-reflection coating, 75 nm of magnesium fluoride (MgF_2) was thermally evaporated on the glass side.

Sample preparation for AFM measurement. The replicate of perovskite surface were fabricated using a one-step soft lithographic replication process, similar to that reported in Ref. [2] The silicone elastomer base and its curing agent (Sylgard 184) were purchased from Dow Corning. The reagents were mixed at a ratio 10:1 (w/w) and degassed for about an hour to prepare the cross-linking silicone elastomer which were then poured onto the perovskite film. After curing for 1 day, the implied perovskite films were obtained by peeling the silicone gel off the perovskite surface.

Characterization. Dynamic light scattering (DLS) measurements were carried out by Zetasizer Nano ZS. The measurement was done with a quartz cuvette at room temperature. Top view and cross-sectional SEM images were obtained using a field emission SEM (NanoSEM 230) in vacuum. X-ray diffraction (XRD) patterns were measured using a PANalytical Xpert Materials Research diffractometer system with a Cu Kα radiation source ($\lambda = 0.1541$ nm) at 45 kV and 40 mA in air. The sample was sealed in a dome air-sealed holder during the measurement. AFM measurements were performed on implied perovskite films to evaluate surface roughness using Bruker Dimension ICON SPM. X-ray photoelectron spectroscopy (XPS) study was carried using the Thermo ESCALAB250Xi X-ray photoelectron spectrometer. The optical reflection and transmission spectra were measured using Cary spectrophotometer and the test samples are encapsulated with PIB. The time-resolve PL (tr-PL) decay traces were measured by the Microtime-200 (PicoQuant) with 470 nm excitation and detection through a 620/40 nm band pass filter.The current density–voltage (J–V) measurements were performed using a solar cell I–V testing system from PV Measurements Inc. under an illumination power of 100 mW cm^{-2} with an 0.159 cm^2 aperture

and a scan rate at 0.02 Vs^{-1}. All devices have been light soaked for 30 minutes before the J-V measurement. For stability tests, the encapsulated devices are stored in the dark at room temperature with relative humidity between 50-70 %, as shown in Figure S9. The external quantum efficiency (EQE) was measured using the PV Measurement QXE7 spectral response system with monochromatic light from a xenon arc lamp. Both J-V and EQE measurements were undertaken on encapsulated devices at room temperature in ambient condition.

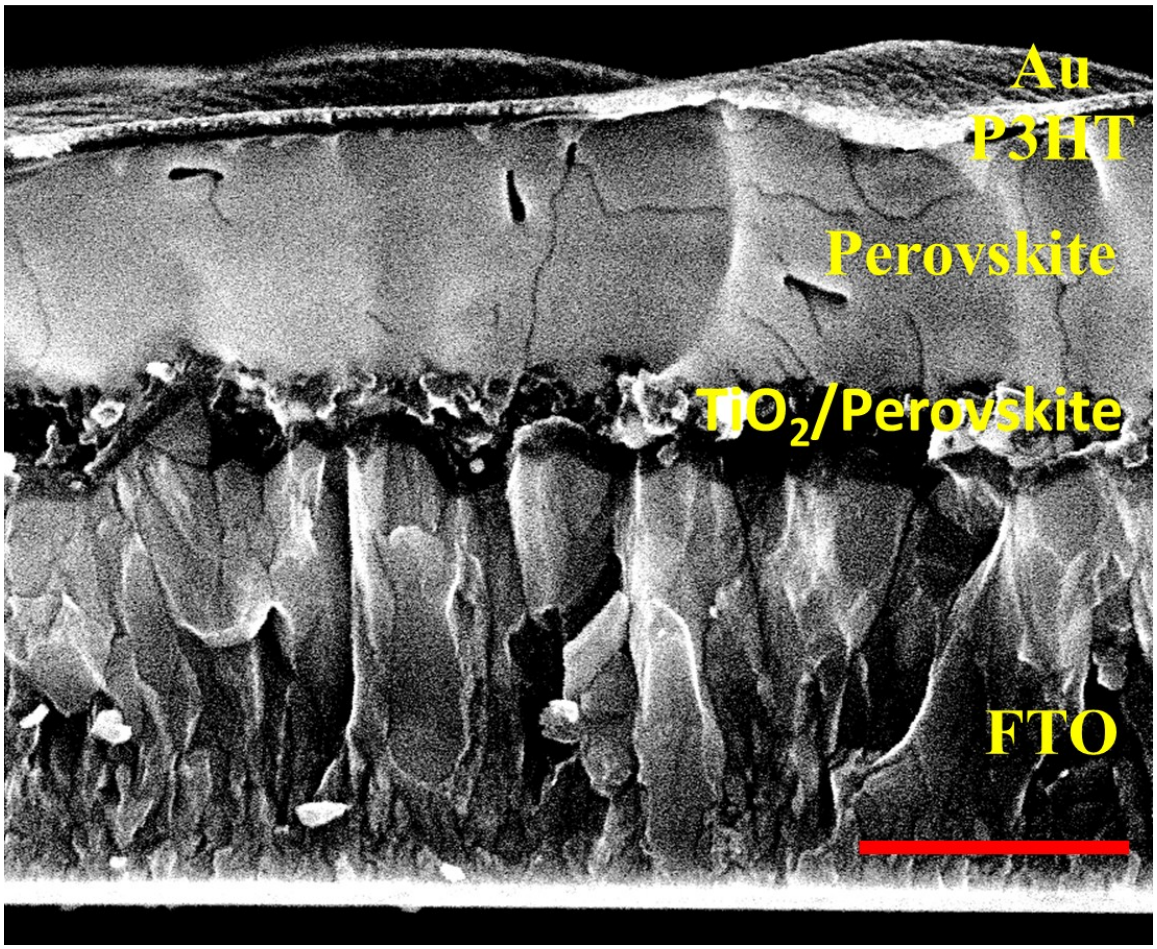

Figure S1. Cross-sectional SEM image of a typical FTO/c-TiO2/mp-TiO_2/$CsPb_{1-x}Ca_xI_3$/P3HT/Au where x is the molar ratio of Ca in the precursor. Scale Bar: 500 nm

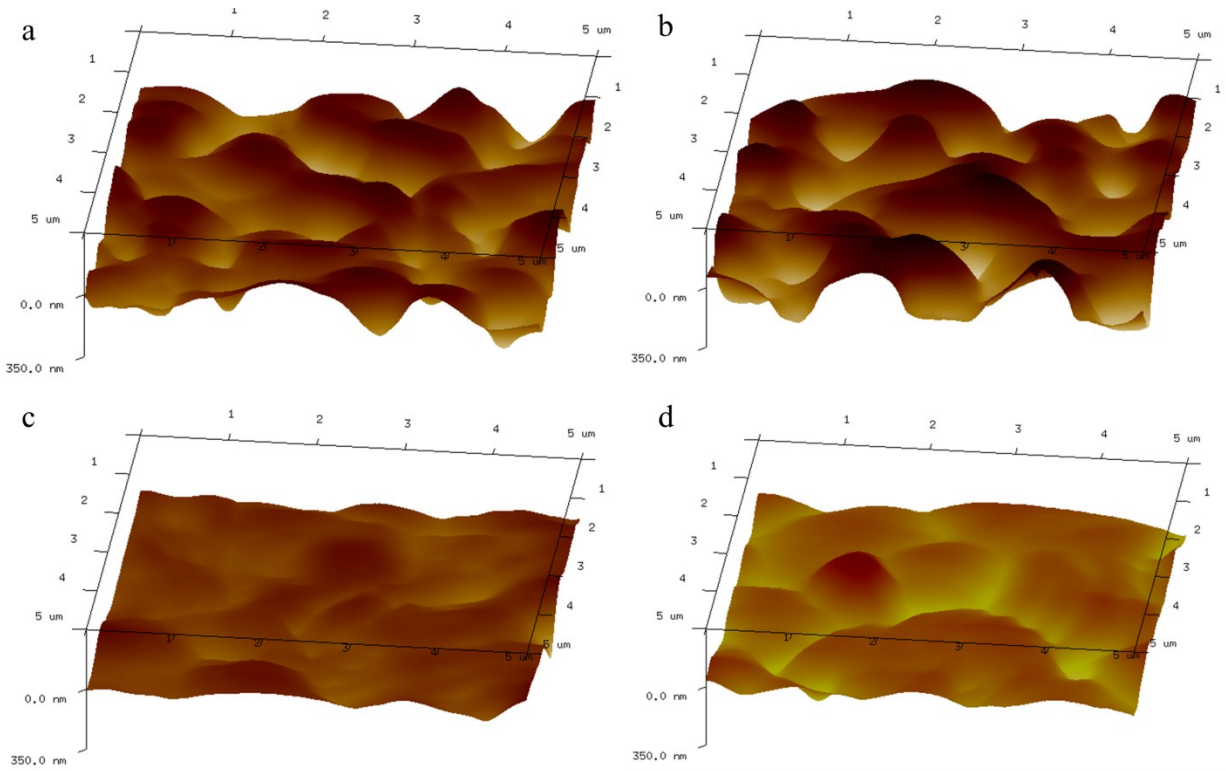

Figure S2. 3-dimensional AFM images of the implied $CsPb_{1-x}Ca_xI_3$ perovskite film where *x* is the molar ratio of Ca in the precursor solution (a) $CsPbI_3$, (b) $CsPb_{0.98}Ca_{0.02}I_3$, (c) $CsPb_{0.95}Ca_{0.05}I_3$, and (d) $CsPb_{0.93}Ca_{0.07}I_3$.

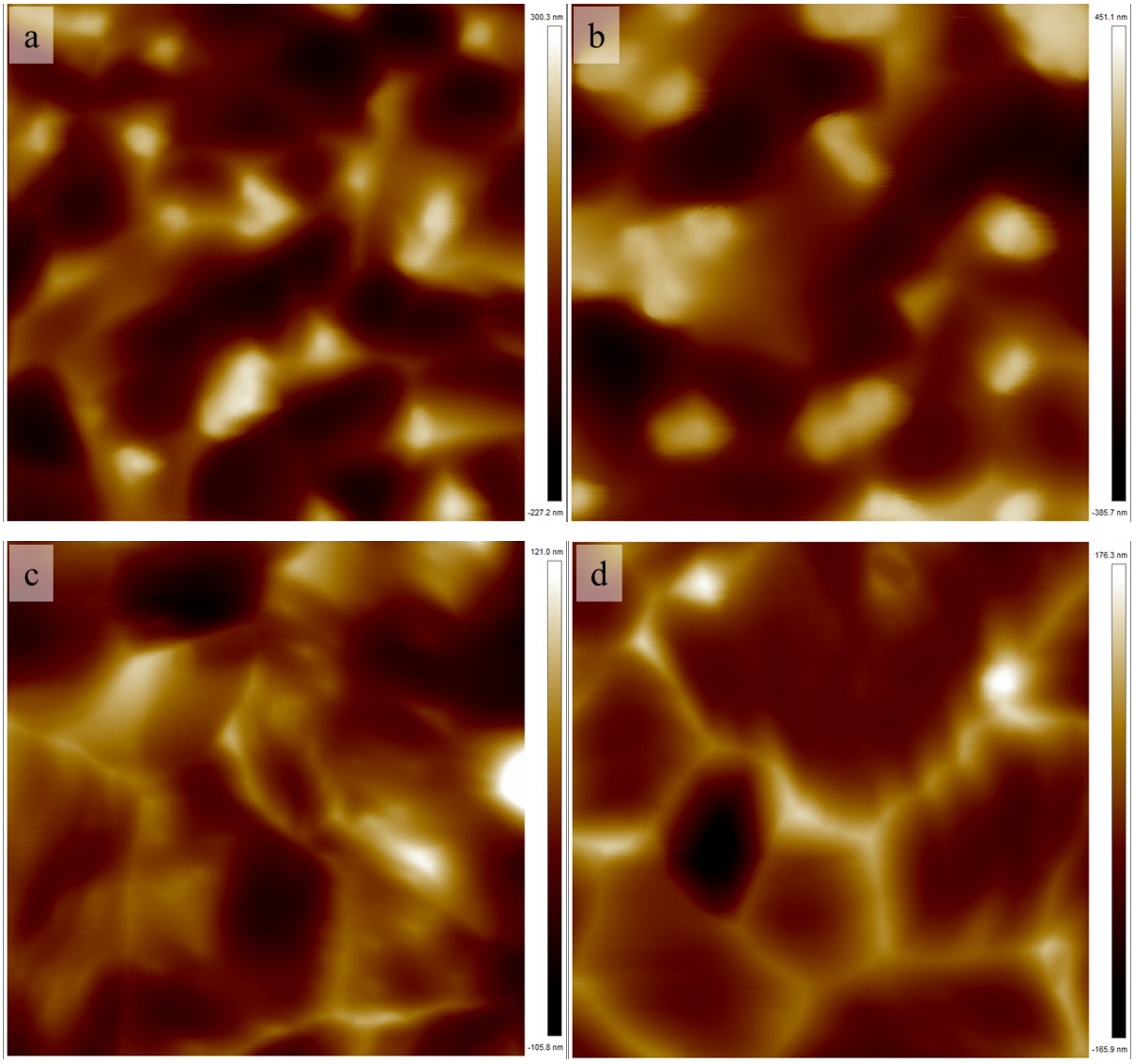

Figure S3. Top-view AFM images of implied $CsPb_{1-x}Ca_xI_3$ perovskite film where x is the molar ratio of Ca in the precursor solution (a) $CsPbI_3$, (b) $CsPb_{0.98}Ca_{0.02}I_3$, (c) $CsPb_{0.95}Ca_{0.05}I_3$, and (d) $CsPb_{0.93}Ca_{0.07}I_3$.

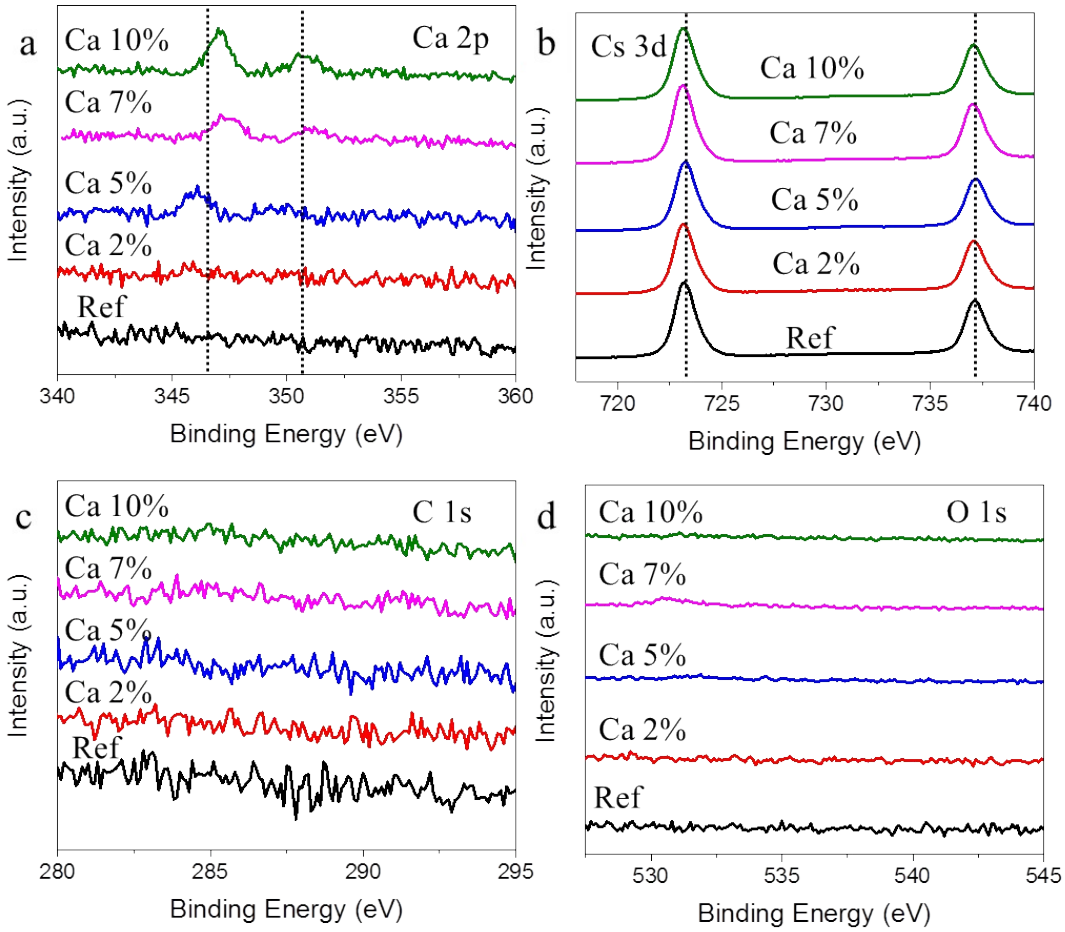

Figure S4. XPS spectra for (a) Ca 2p, (b) Cs 3d, (c) C 1s, (d) C 1s, and (e) O 1s 50nm into the perovskite film fabricated using $CsPb_{1-x}Ca_xI_3$ precursor solution.

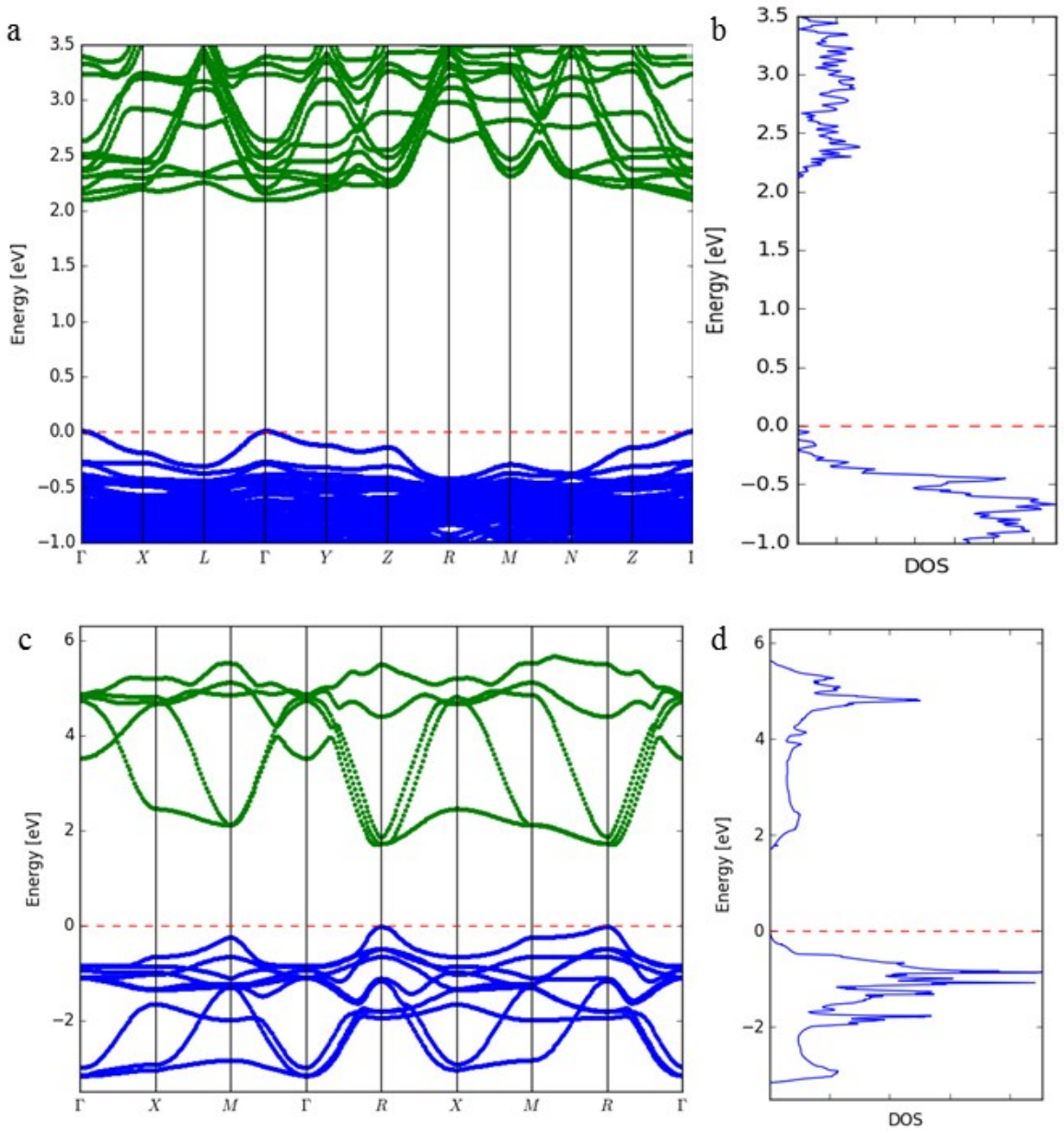

Figure S5. Ab-initio simulation of the (a, c) electronic band-structure and (b, d) density of states for a 2x2x2 $CsPb_{0.875}Ca_{0.125}I_3$ (x=0.125) and $CsPbI_3$ supercell, respectively, produced using the Projector augmented wave (PAW) method.

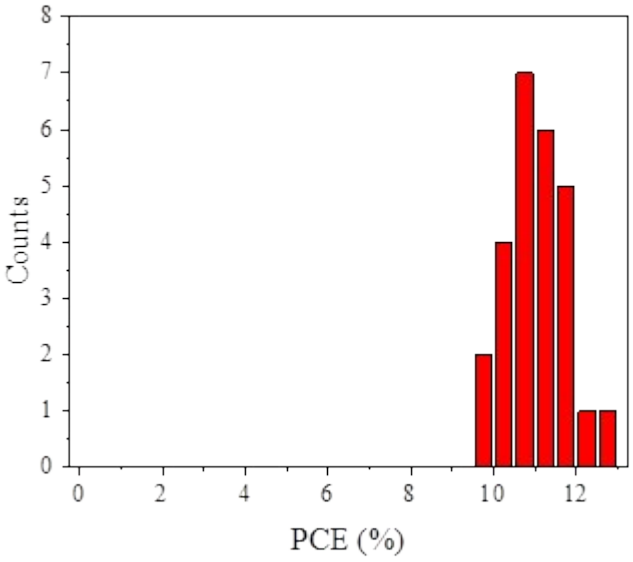

Figure S6. Distributions of reverse scan PCE of 26 perovskite devices fabricated using 5% Ca^{2+} substitution in the precursor solution.

Table S1. Photovoltaic parameters (with standard deviations) of perovskite devices as a function of Ca^{2+} concentration in the perovskite precursor solution. Numbers in brackets are champion device parameters as shown in Figure 7a in the manuscript.

	PCE (%)	J_{SC} (mA/cm^2)	V_{OC} (mV)	FF (%)
Reference	9.4 ± 0.83 (10.6)	17.4 ± 0.47 (17.1)	790 ± 64.2 (853)	68.7 ± 4.36 (72.6)
2% Ca	9.0 ± 0.77 (9.72)	18.1 ± 0.83 (17.9)	752 ± 35.5 (828)	65.4 ± 4.07 (65.7)
5% Ca	11.0 ± 0.74 (12.6)	17.1 ± 0.38 (17.3)	881 ± 27.3 (940)	73.0 ± 3.52 (77.7)
7% Ca	9.8 ± 0.34 (10.4)	16.1 ± 0.15 (16.0)	833 ± 49.2 (882)	73.4 ± 2.29 (73.9)
10% Ca	8.6 ± 1.29 (10.6)	15.1 ± 0.57 (15.2)	832 ± 84.4 (914)	68.2 ± 6.54 (76.0)
15% Ca	6.74 ± 0.39 (7.16)	13.6 ± 0.57 (12.8)	769 ± 32.6 (790)	64.5 ± 3.35 (69.8)

Table S2 Summary of high performance of the $CsPbI_3$ based PSCs.

Device structure	**Material**	V_{oc} **(V)**	J_{sc} **(mA/cm²)**	***FF*** **(%)**	**PCE (%)**	**Scan Direction**	**Ref**
ITO/PEDOT:PSS/$CsPbI_3$/PCBM/Al	$CsPbI_3$	0.79	0.3	45	0.3	V_{OC}->J_{SC}	[3]
FTO/c-TiO_2/$CsPbI_3$/Spiro/Au		0.80	12.0	30	2.9	V_{OC}->J_{SC}	[4]
FTO/c-TiO_2/mp-TiO_2/$CsPbI_3$/P3HT/MoO_3/Au		0.67	11.3	61	4.6	V_{OC}->J_{SC}	[5]
FTO/c-TiO2/CsPbI3/Spiro/Ag		0.65 0.62	12.2 11.9	44 31.3	3.5 2.3	V_{OC}->J_{SC} J_{SC} ->V_{OC}	[6]
ITO /Ca /C60/$CsPbI_3$ /TAPC/TAPC:MoO_3/Ag					9.4	?	[7]
FTO/c-TiO_2/$CsPbI_3$/P3HT/Au		1.06 0.99	13.8 13.9	72 68	10.5 9.3	V_{OC}->J_{SC} J_{SC} -> V_{OC}	[8]
FTO/c-TiO_2/$CsPbI_3$/Spiro/Au		0.55	0.5	44.2	0.1	V_{OC}->J_{SC}	[9]
FTO/c-TiO_2/$CsPbI_3$/P3HT/Au		0.71	12.1	67	5.7	?	[10]
FTO/SnO_2/$CsPbI_3$/Carbon nanotubes/Spiro/Au		1	13.0	68	8.8 7.8	V_{OC}->J_{SC} Stabilized	[11]
FTO/c-TiO_2/$CsPbI_3$/P3HT/Ag		12.06	0.8	72	6.8	?	[12]
FTO/c-TiO_2/$CsPb_{0.96}Bi_{0.04}I_3$/CuI/Au	$CsPb_{0.96}Bi_{0.04}I_3$	0.97	18.8	72.9	13.2 13.2	V_{OC}->J_{SC} Stabilized	[13]
FTO/c-TiO2/ $CsPbI_3$·0.025EDAPbI_4/Spiro-OMeTAD/Ag	$CsPbI_3$·0.025EDAPbI_4	1.15	14.5	71	11.9	V_{OC}->J_{SC}	[14]
MgF_2/glass/FTO/c-TiO_2/mp-TiO_2/ $CsCa_{0.05}Pb_{0.95}I_3$ /P3HT/Au	**$CsCa_{0.05}Pb_{0.95}I_3$ in precursor**	**0.95**	**17.9**	**80**	**13.5 13.3**	**V_{OC}->J_{SC} Stabilized**	**This work**

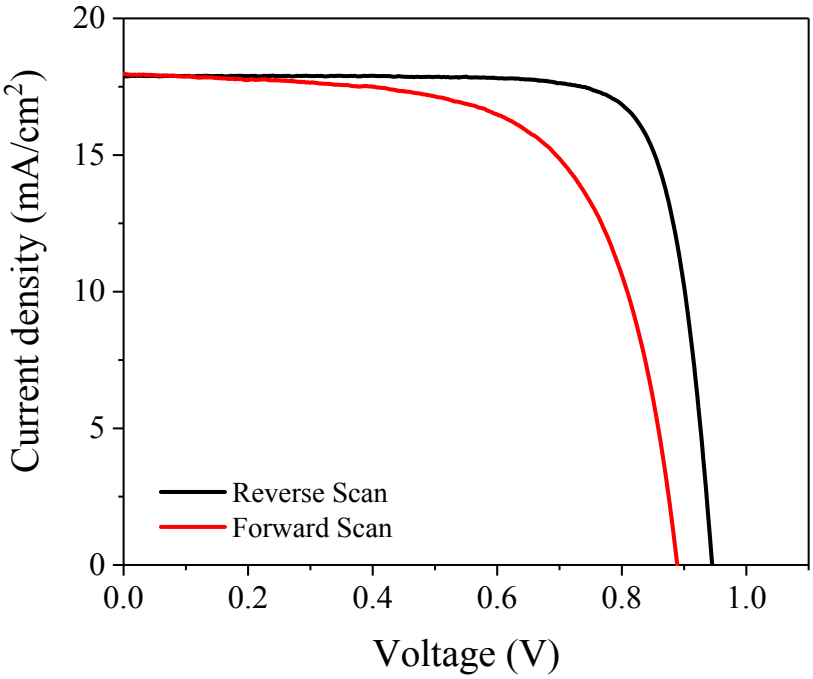

Figure S7. Light J–V characteristics of champion Cs perovskite devices using $CsPb_{0.98}Ca_{0.02}I_3$ precursor under forward and reverse scans.

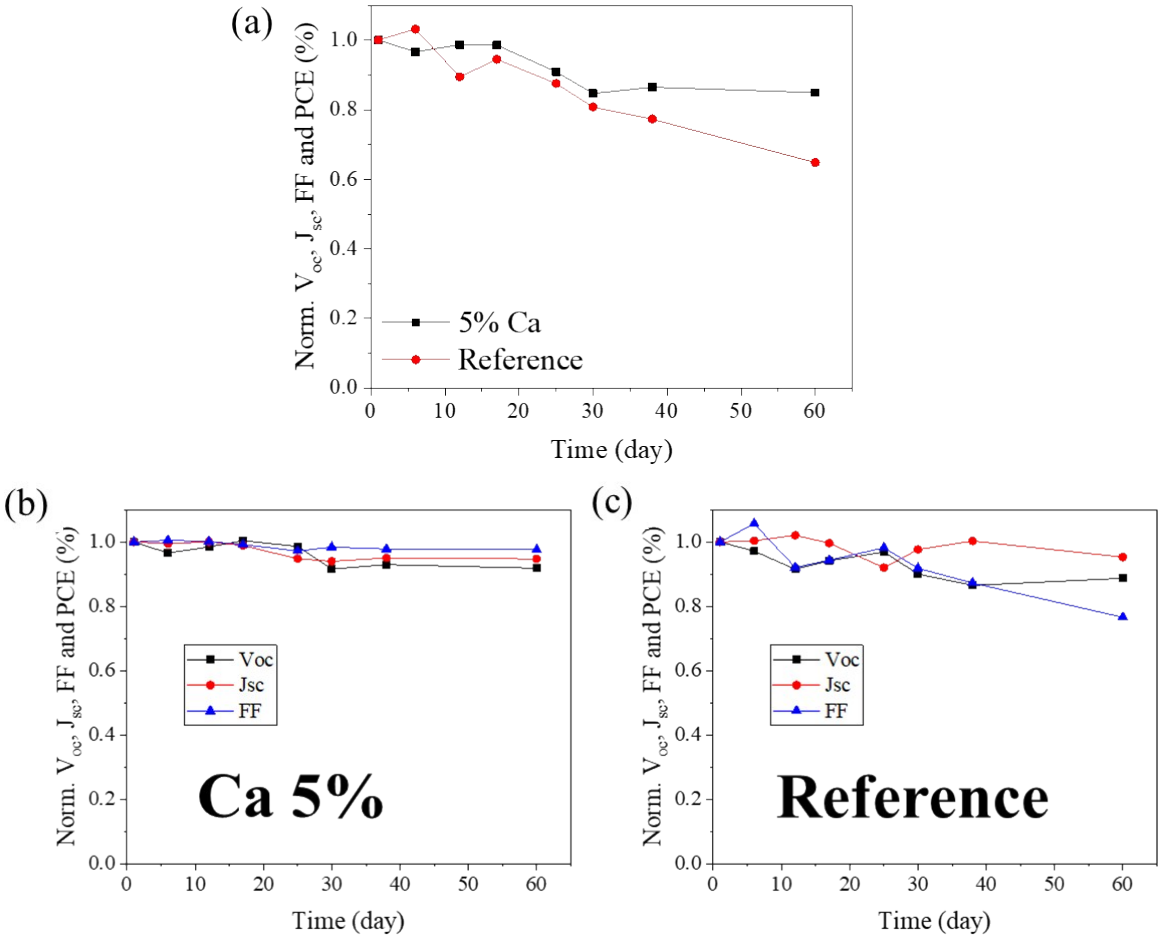

Figure S8. (a) Normalized PCE for encapsulated 5% Ca and 0% Ca CsPb1-xCaxI3 devices (x is the molar ratio in the precursor) as a function of storage time in the dark at room temperature with relative humidity between 60-70%. Normalised VOC, JSC and FF of the (b) 5% Ca and (c) 0% Ca device.

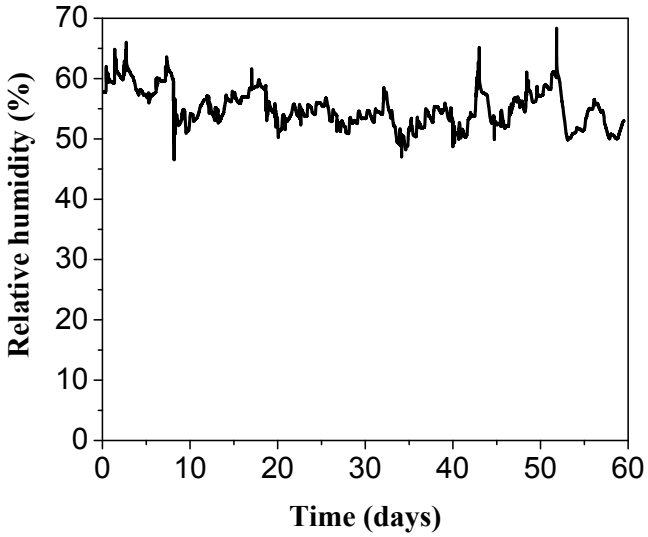

Figure S9. Relative humidity of ambient in which perovskite devices were stored

[1] L. Shi, T. L. Young, J. Kim, Y. Sheng, L. Wang, Y. Chen, Z. Feng, M. J. Keevers, X. Hao, P. J. Verlinden, M. A. Green, A. W. Y. Ho-Baillie, *ACS Appl. Mater. Interfaces* **2017**, *9*, 25073.

[2] K. Li, Y. Zhang, H. Zhen, H. Wang, S. Liu, F. Yan, Z. Zheng, *J. Mater. Chem. A* **2017**, *5*, 969.

[3] H. Choi, J. Jeong, H. B. Kim, S. Kim, B. Walker, G. H. Kim, J. Y. Kim, *Nano Energy* **2014**, *7*, 80.

[4] G. E. Eperon, G. M. Paternò, R. J. Sutton, A. Zampetti, A. A. Haghighirad, F. Cacialli, H. J. Snaith, *J. Mater. Chem. A* **2015**, *3*, 19688.

[5] T. S. Ripolles, K. Nishinaka, Y. Ogomi, Y. Miyata, S. Hayase, *Sol. Energy Mater. Sol. Cells* **2016**, *144*, 532.

[6] P. Luo, W. Xia, S. Zhou, L. Sun, J. Cheng, C. Xu, Y. Lu, *J. Phys. Chem. Lett.* **2016**, *7*, 3603.

[7] C. Chen, H. Lin, K. Chiang, W. Tsai, Y. Huang, C. Tsao, H. Lin, *Adv. Mater.* **2017**, *29*, 1.

[8] L. A. Frolova, D. V. Anokhin, A. A. Piryazev, S. Y. Luchkin, N. N. Dremova, K. J. Stevenson, P. A. Troshin, *J. Phys. Chem. Lett.* **2016**, 67.

[9] J.-F. Liao, H.-S. Rao, B.-X. Chen, D.-B. Kuang, C.-Y. Su, *J. Mater. Chem. A* **2017**, *5*, 2066.

[10] K. Yonezawa, K. Yamamoto, M. Shahiduzzaman, Y. Furumoto, K. Hamada, T. S. Ripolles, M. Karakawa, T. Kuwabara, K. Takahashi, S. Hayase, T. Taima, *Jpn. J. Appl. Phys.* **2017**, *56*, 04CS11.

[11] E. M. Hutter, R. J. Sutton, S. Chandrashekar, M. Abdi-Jalebi, S. D. Stranks, H. J. Snaith, T. J. Savenije, *ACS Energy Lett.* **2017**, *2*, 1901.

[12] M. Shahiduzzaman, K. Yonezawa, K. Yamamoto, T. S. Ripolles, M. Karakawa, T. Kuwabara, K. Takahashi, S. Hayase, T. Taima, *ACS Omega* **2017**, *2*, 4464.

[13] Y. Hu, F. Bai, X. Liu, Q. Ji, X. Miao, T. Qiu, S. Zhang, *ACS Energy Lett.* **2017**, 2219.

[14] T. Zhang, M. I. Dar, G. Li, F. Xu, N. Guo, M. Grätzel, Y. Zhao, *Sci. Adv.* **2017**, *3*, 1.